Evaluating estimation methods for wildfire smoke and their implications for assessing health effects

Minghao Qiu [1,2,*], Makoto Kelp [1], Sam Heft-Neal [3], Xiaomeng Jin [4], Carlos F. Gould [5], Daniel Q. Tong [6], Marshall Burke [1,3,7]

1 Doerr School of Sustainability, Stanford University, Stanford, CA, USA

2 Center for Innovation in Global Health, Stanford University, Stanford, CA, USA

3 Center on Food Security and the Environment, Stanford University, Stanford, CA, USA

4 Department of Environmental Sciences, Rutgers University, New Brunswick, NJ, USA

5 School of Public Health, University of California San Diego, La Jolla, CA, USA

6 Department of Atmospheric, Oceanic and Earth Sciences, George Mason University, Fairfax, VA, USA

7 National Bureau of Economic Research, Cambridge MA, USA

* To whom correspondence should be addressed. E-mail: mhqiu@stanford.edu

Abstract

Growing wildfire smoke represents a substantial threat to air quality and human health in the US and across much of the globe. However, the impact of wildfire smoke on human health remains imprecisely understood, due to uncertainties in both the measurement of population wildfire smoke exposure and dose-response functions linking exposure to health. Here, we compare daily wildfire smoke-related surface fine particulate matter ($PM_{2.5}$) concentrations estimated using three approaches, including two chemical transport models (CTMs): GEOS-Chem and Community Multiscale Air Quality (CMAQ), and one machine learning (ML) model over the contiguous US in 2020, a historically active fire year. We study the consequences of these different approaches for estimating smoke $PM_{2.5}$ concentrations and the effects of smoke $PM_{2.5}$ on mortality. In the western US, compared against surface $PM_{2.5}$ measurements from US Environmental Protection Agency (EPA) and PurpleAir sensors, we find that CTMs overestimate $PM_{2.5}$ concentrations during extreme smoke episodes by up to 3-5 fold, while ML estimates are largely consistent with surface measurements. However, in the eastern US, where smoke levels were much lower in 2020, CTMs show modestly better agreement with surface measurements. We develop a calibration framework that integrates CTM- and ML-based approaches and yields estimates of smoke $PM_{2.5}$ concentrations that outperform each individual approach. When combining the estimated smoke $PM_{2.5}$ concentrations with county-level mortality rates, we find consistent effects of low-level smoke on mortality but large discrepancies on the effects of high-level smoke exposure across different methods. Our research highlights the benefits and costs of different estimation methods for understanding the health impacts of wildfire smoke, and demonstrates the importance of bench-marking estimates with available surface measurements.

Introduction

Wildfires and the smoke they generate pose a substantial threat to the environment and public health globally. In the United States, wildfire burned area has more than quadrupled over the last three decades (*1*), largely driven by human-induced climate change (*2–4*), historical fire suppression (*5*), and the expansion of human activities into forested areas (*6*). Increased wildfire activity and associated smoke emissions have also contributed to significant increases in ambient air pollution (specifically fine particulate matter, $PM_{2.5}$) (*7–10*). In many parts of the western US, recent estimates suggest that wildfire smoke $PM_{2.5}$ has accounted for over 50% of the annual concentration of $PM_{2.5}$ in extreme smoke years (*11*, *12*), and has led to stagnation or even reversal of the otherwise declining trend in ambient $PM_{2.5}$ over the last two decades (*13*). As a result of increased wildfire risks under future climate change, wildfire smoke pollution and the associated health burdens are projected to increase substantially in the US in the coming decades (*14–17*).

While accumulating evidence suggests that exposure to wildfire smoke $PM_{2.5}$ can negatively impact physical and mental health outcomes, large uncertainties remain in estimating the mortality and disease burden attributable to wildfire smoke (*18*, *19*). Such uncertainty is a result of 1) the difficulty in estimating pollutant concentrations associated with wildfire smoke (and thus population exposures), and 2) the uncertainty of derived dose-response functions that relate wildfire smoke to various health outcomes. For instance, existing work has shown that estimates of $PM_{2.5}$ enhancement due to the same wildfire events can differ dramatically depending on the data and models used in the process (*20*, *21*), which ultimately lead to widely different estimates of health burdens. The broader literature on the health impacts of wildfire smoke exposure remains similarly mixed (*18*, *19*, *22*), perhaps in part related to methodological challenges in modelling wildfire-specific $PM_{2.5}$ exposure (*23*). For example, previous studies have shown both positive, negative, and no associations between smoke $PM_{2.5}$ and cardiovascular outcomes (*19*, *24*), in contrast to robustly identified effects of total $PM_{2.5}$ on cardiovascular mortality and morbidity (*25*). Compared to total all-source $PM_{2.5}$, modelling wildfire smoke $PM_{2.5}$ concentrations is more challenging due to the lack of benchmark measurements, as surface monitors only measure $PM_{2.5}$ concentrations in the ambient atmosphere which include contributions from fire and non-fire sources, and because wildfire smoke emissions and concentrations change more dynamically across space and time.

Broadly speaking, researchers have used two approaches to estimate wildfire smoke impacts on surface $PM_{2.5}$. One widely-used approach is mechanistic atmospheric chemical transport models (CTM) that simulate the effects of wildfires on surface $PM_{2.5}$. Studies often use CTMs paired with wildfire emissions inventories to simulate two scenarios: one including wildfire emissions and one excluding wildfire emissions. They then attribute the differences between the two scenarios as the estimated wildfire smoke $PM_{2.5}$ concentrations. Wildfire smoke $PM_{2.5}$ simulated by CTMs are widely used in epidemiological studies to estimate dose-response functions (*26–28*) and to quantify health burdens due to wildfire smoke (*17*, *26*, *29*, *30*). However, the estimated wildfire smoke $PM_{2.5}$ from CTMs is subject to uncertainty in emission inventories (*31*, *32*), plume rise (*20*, *33*), and fire-weather interactions (*34*), which results in modeled smoke concentrations potentially differing by an order of magnitude when compared to surface observations (*35*, *36*). Some studies have calibrated CTM outputs against available surface measurements to correct for their potential biases before using them in downstream health impacts analysis (*37*), but such practices have not been widely adopted.

Another increasingly popular approach is to use statistical and machine learning (ML) methods to characterize the relationship between input variables (such as remotely sensed atmospheric variables, meteorology, and fire information) and $PM_{2.5}$ measured at surface monitors during wildfire episodes. CTM outputs are sometimes also used as input features for predicting surface $PM_{2.5}$ concentrations (*38*). By applying such a relationship to locations without surface monitors, these studies can generate wildfire smoke estimates continuously in space and time (similar to CTMs). Prior studies have used various statistical algorithms of different complexity (*23*, *39*, *40*). More recently, ML methods have been used to estimate wildfire smoke concentrations (*9*, *10*, *41*). Similar to CTM outputs, wildfire smoke $PM_{2.5}$ generated by these statistical methods are widely used for establishing dose-response functions and assessing the overall health effects of wildfire smoke (*14*, *42–45*).

Despite the popularity of CTM and ML methods for quantifying the health impacts of wildfire smoke, little are known about the implications and influence of the different wildfire smoke estimation approaches for downstream health impact assessment. Previous studies have quantified the performance and uncertainty of each approach (often by comparing against surface observations) or compared CTMs to other non-ML approaches (*23*, *38*, *46–49*). However, to our knowledge, there is no inter-comparison between CTM and the increasingly popular ML approaches in terms of their ability to predict wildfire smoke $PM_{2.5}$. More importantly, for downstream users of these datasets, very little is known about the differences in the established dose-response functions and health burdens across the different smoke estimation methods. Differences across wildfire smoke $PM_{2.5}$ datasets can affect estimated health burdens in two ways. First, when applied to an existing dose-response function, disparity in smoke exposure can lead to widely different attributed health impacts. Second, the use of smoke $PM_{2.5}$ data to estimate novel dose-response relationships can yield biased estimates of these relationships if the smoke $PM_{2.5}$ are themselves estimated with error. In a case study that evaluated the effects on hospitalizations in Washington State over a four-month period, Gan et al. demonstrated that the choice of wildfire estimation methods can generate different health impact estimates across CTM, spatial interpolation, and regression methods (*23*). Better understanding the potential measurement error associated with leading smoke estimation approaches to estimating smoke $PM_{2.5}$, and the implications for estimating dose-response functions and health burdens, is essential for quantifying the health impacts of wildfire smoke, and for informing researchers on how to best use the wildfire smoke datasets for health impact analysis.

Here, we compare the estimated daily wildfire smoke $PM_{2.5}$ in 2020 over the contiguous US using two CTMs (GEOS-Chem and Community Multiscale Air Quality Model (CMAQ)) and one ML model. Figure 1 shows an overview of our research methods. For the GEOS-Chem CTM, we simulate two scenarios, a baseline scenario that includes wildfire emissions derived from the fourth version of the Global Fire Emissions Database with small fires (GFED4s) (*50*), and a no-fire scenario that excludes wildfire emissions. For the CMAQ CTM, we use daily wildfire smoke $PM_{2.5}$ archived in (*11*). For ML estimates, we use the daily smoke $PM_{2.5}$ from (*9*). All three estimates are compared to surface $PM_{2.5}$ concentrations measured by EPA reference-grade monitors and PurpleAir sensors. We design two methods for evaluating the performance of the three estimation approaches: 1) directly comparing to anomalous increases of surface $PM_{2.5}$ at monitors when smoke plumes are overhead, and 2) comparing to total $PM_{2.5}$ measurements after adding estimated smoke $PM_{2.5}$ to the same non-smoke $PM_{2.5}$ estimates. To ensure fair comparisons between CTM and ML approaches, we use ML model predictions obtained from held-out monitor locations that were not used in model training. We then develop a calibration framework that integrates the three individual estimates to generate improved smoke $PM_{2.5}$ estimates.

Finally, we empirically estimate the effects of annual smoke $PM_{2.5}$ concentration, derived from the calibrated model and three individual methods, on annual mortality rates using county-level data from 2006 to 2020 on all recorded deaths in the US. Due to data availability, we combine the ML estimates from 2006-2019 and the estimates from each method in 2020. Thus, our approach only quantifies the differences in the dose-response functions due to one year of wildfire smoke data coming from different estimation methods. Finally, we calculate the smoke-related excess deaths across the calibrated model and three individual methods, using both the dose-response function derived as described above for each method as well as smoke-specific dose-response functions documented in prior literature.

Methods

Chemical transport models

We use GEOS-Chem version 14.0.2 (https://doi.org/10.5281/zenodo.1343546) driven by assimilated meteorological data from the NASA Global Modeling and Assimilation Office (GMAO). GEOS-Chem computes the evolution of atmospheric composition by a successive application over model time steps of the operators simulating emissions, transport, chemistry, and deposition (*51*). Here, we conduct nested simulations at 0.25°× 0.3125°horizontal resolution over the North America domain (140°W–40°W, 10°N–70°N) using the GEOS forward processing (GEOS-FP) meteorological data set. Chemical boundary conditions at the edges of the nested domain are updated every 3-h from

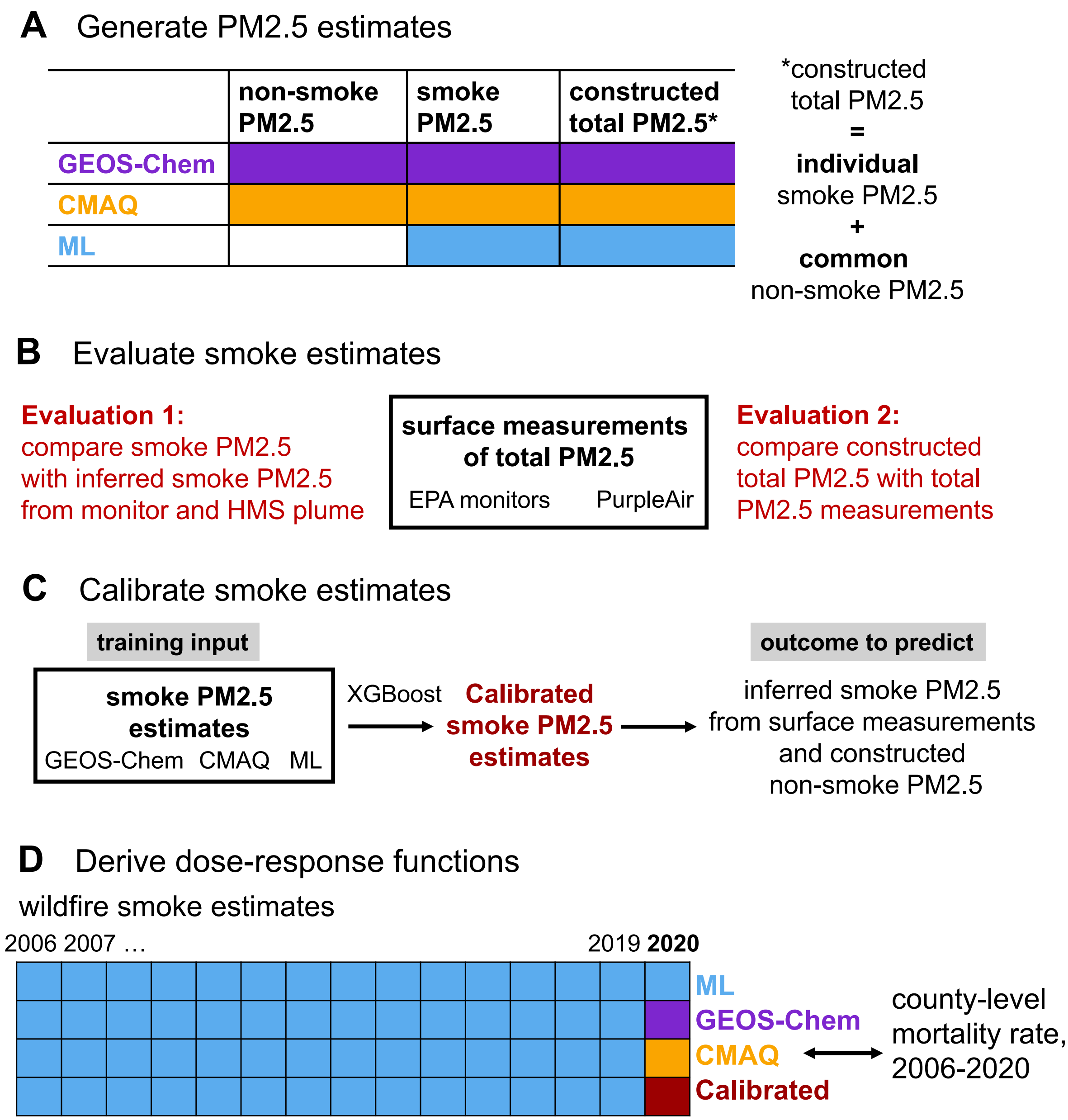

Figure 1: Schematic figure of the research methodology.

a global simulation with 4°× 5°resolution. We conduct a simulation for 2020 (January-November) with 6 months of initialization. We use emissions estimates from the GFED4s with a spatial resolution of 0.25°× 0.25°(*50*). The fire emissions are based on satellite-derived burned area, fuel load computed using the Carnegie-Ames-Stanford-Approach biogeochemical model, and estimated emission factors of aerosol and trace gases from each biome type from (*52*). In the simulation, we use daily emissions estimated from monthly GFED4s emissions and daily active fire detection (*53*). We run two scenarios to estimate wildfire effects on surface $PM_{2.5}$: 1) with GFED4s emissions turned on simulating fire smoke in North America, and 2) with GFED4s turned off which produces a "no smoke" control.

By default, GEOS-Chem distributes biomass burning emissions uniformly within the boundary layer. To test the influence of injection heights and alternative emission inventory on the simulated $PM_{2.5}$ concentrations in GEOS-Chem, we further perform three sensitivity simulations over California (latitude: 27°N-47°N, longitude: 110°W-130°W) that: (1) distributes 65% of the biomass burning emissions within the boundary layer and the other 35% of emissions in the first ten sigma layers above the boundary layer following (*54*); (2) distributes 5% of the biomass burning emissions within the boundary layer and 95% biomass burning emissions in the first ten sigma layers above the boundary layer; (3) use CAMS Global Fire Assimilation System (GFAS) based on satellite observed fire radiative power (*55*) with dynamic injection heights (*56*).

We also use the Community Multiscale Air Quality Model (CMAQ), another widely-used CTM to quantify $PM_{2.5}$ enhancements due to wildfire smoke in 2020. We use the model output archived from Li et al., 2021 (*11*). Li et al. used the CMAQ model version v5.3.1 to simulate daily surface $PM_{2.5}$ at a spatial resolution of 12km for one scenario including wildfire emissions and one scenario excluding them. The CMAQ simulation used the biomass burning emission inventory from GBBEPx v3 system (*57*) and the injection height scheme from (*58*) based on a previous evaluation of 8 combinations of biomass burning emission inventory and injection height schemes (*59*). GBBEPx v3 system estimates daily global biomass burning emissions at 0.1 degree or 3km resolution using fire radiative power from a suite of satellite products, using the same algorithm as Quick Fire Emissions Data set (QFED). More details about the CMAQ simulation can be found in (*11*). All CTM outputs are regridded at 10km resolution to be comparable to the ML output (see below).

Machine learning estimates of smoke $PM_{2.5}$

We use gridded daily wildfire smoke $PM_{2.5}$ predictions for the contiguous US at 10 km resolution from January 1, 2006 to November 30, 2020 derived from (*9*). Childs et al. constructed a ML model that uses satellite-derived smoke plume data, remotely-sensed atmospheric variables, and meteorological variables to predict the anomalous increases in surface $PM_{2.5}$ measured by surface air quality monitors during wildfire. Their model achieved a R^2 of 0.67 when evaluated against held-out samples at the daily monitor level. The dataset has been widely used for establishing dose-response functions and assessing the overall health effects of wildfire smoke (*14*, *42*, *43*).

The ML model in (*9*) was trained to predict surface $PM_{2.5}$ data measured at EPA sensors, and thus direct comparisons between the ML model outputs and surface measurements could lead to inflated performance. To address this issue, we use the out-of-sample predictions from their machine learning algorithm for grid cells that contain EPA sensors. In other words, predicted smoke concentrations in those grid cells are derived from a model trained on a sample that excludes monitor measurements in that grid cell. For grid cells with only PurpleAir sensors and no EPA sensors, we directly use the output from Childs et al. as PurpleAir data was not used in the original model training.

Surface measurements of $PM_{2.5}$

We use surface $PM_{2.5}$ measurements derived from the reference-grade sensors administered by the US EPA as well as measurements from low-cost PurpleAir sensors. Our final data includes 373,203 daily measurements from 1,276 EPA sensors, and 1.3 million daily measurements from 6,553 PurpleAir sensors. Surface $PM_{2.5}$ concentrations are derived from the US Air Quality Systems administered by the US EPA (*60*), and all publicly reporting outdoor PurpleAir monitors in the US. We first regrid surface measurements at the 10km grid cell level to be consistent with the wildfire smoke estimates, and calculate the daily mean concentration for each grid cell over the EPA and PurpleAir sensors separately. If one grid cell has both EPA and PurpleAir sensors, we then take their average as the daily mean concentration for that grid cell. We drop all observations with negative daily $PM_{2.5}$ concentrations (<0.5% of our full data). One thing to note is that samplers used in certain surface monitors can get clogged due to overload of smoke (*61*). We use all measurements that are available on the Air Quality Systems website, but the malfunctioning monitors during extreme wildfire smoke could influence our evaluations.

For PurpleAir sensors, we only use measurements from outdoor sensors in 2020. The raw temporal resolution of measurements is 10 minutes, and we temporally aggregate them to the daily level after removing unrealistic 10-minute observations (*62*). Prior studies have found that PurpleAir sensors can generally characterise enhancements of surface $PM_{2.5}$ due to wildfire smoke, yet the quantitative magnitude needs to be calibrated to match measurements obtained from reference-grade air quality monitors (*63*). We use the method from Barkjohn et al. to calibrate the raw daily concentrations from PurpleAir sensors for wildfire conditions (*64*). Following PurpleAir guidelines, we then drop all measurements with a daily mean concentration above 1,000 $\mu g/m^3$ and top-code all concentrations at 500 $\mu g/m^3$ if the raw concentrations are in the range of 500-1,000 $\mu g/m^3$. Only 96 records from 25 sensors are either dropped or top-coded at 500 $\mu g/m^3$ out of 1.3 million records in our sample.

We combine surface measurements of $PM_{2.5}$ with satellite-derived smoke plume data to calculate the anomalous increases in surface $PM_{2.5}$ due to wildfire smoke, following similar approaches from (*8*, *9*). The smoke plume data is derived from the National Oceanic and Atmospheric Administration (NOAA) Hazard Mapping System (HMS), which includes analyst-identified plume boundaries based on visible bands of satellite imagery (*65*). For any given monitor, we determine a day to be "smoke day" if identified plume was overhead the monitor location. For any smoke day, we calculate $PM_{2.5}$

anomalies as deviations from recent month- and location-specific non-smoke baselines. For each monitor location, the non-smoke baseline is calculated as the median of all measurements from all non-smoke days that fall in the same month in 2018–2020. The calculated anomalies in surface $PM_{2.5}$ due to wildfire smoke thus consist of zero estimates on all non-smoke days and non-zero deviation on smoke days.

Evaluating wildfire smoke $PM_{2.5}$ estimates using surface measurements

We design two approaches to evaluate the three wildfire smoke $PM_{2.5}$ datasets using surface $PM_{2.5}$ measurements from EPA and PurpleAir sensors:

First, we compare the estimates of smoke $PM_{2.5}$ from three approaches with the inferred smoke $PM_{2.5}$ anomalies for each monitor (Evaluation 1 in Figure 1B). We calculate the root-mean square error (RMSE) between the estimated smoke concentrations and monitor-level anomalies and use it as the evaluation metric. We further evaluate the models' performance under three conditions with different levels of wildfire smoke. "No smoke" includes all monitor days with no smoke plume overhead and low estimated smoke concentrations from both CTMs ($<0.5\ \mu g/m^3$). "Medium and high smoke" includes monitor-days with high estimated smoke $PM_{2.5}$ from both CTMs ($>5\ \mu g/m^3$). "Low smoke" category includes all the other conditions. As we noted above, we use the out-of-sample predictions from the ML model to ensure a fair comparison between surface measurements and the ML model.

Second, we design an evaluation method that uses *total* $PM_{2.5}$ measurements from surface air quality sensors due to the potential uncertainty in the inferred smoke $PM_{2.5}$ anomalies (Evaluation 2 in Figure 1B). As the ML model did not estimate non-smoke $PM_{2.5}$ concentrations, we first create a common non-smoke $PM_{2.5}$ baseline using non-smoke $PM_{2.5}$ simulated by GEOS-Chem and CMAQ:

$$PM^{monitor} = f(PM^{GC}_{nonsmoke}, PM^{CMAQ}_{nonsmoke}, ...) \text{ — only trained on non-smoke days} \quad (1)$$

To do this, we construct a XGBoost ML model (function f in equation 1) to predict total $PM_{2.5}$ measurements during all "non-smoke days" using non-smoke $PM_{2.5}$ simulated by GEOS-Chem and CMAQ as model features. The XGBoost model also uses temperature, precipitation, wind speed, humidity, latitude, longitude, and month-of-year as model features to account for potential seasonal and spatial model biases. Using this model, we then estimate non-smoke $PM_{2.5}$ for all monitor days in our sample (including smoke days). Finally, we calculate three total $PM_{2.5}$ estimates over all monitor locations by adding the different smoke $PM_{2.5}$ estimates to the same non-smoke $PM_{2.5}$ estimated above (Figure 1A). Therefore, the only differences in the three constructed $PM_{2.5}$ series are due to their different estimates of smoke $PM_{2.5}$ as they share the same non-smoke $PM_{2.5}$ estimate. We compare the three constructed total $PM_{2.5}$ series against surface measurements of total $PM_{2.5}$ by calculating RMSE for each monitor location.

Constructing improved wildfire smoke $PM_{2.5}$ estimates by integrating all three sources

Previous work has shown that integrating multiple exposure estimation methods can improve wildfire smoke $PM_{2.5}$ modeling performance (*39*, *48*, *66*). Therefore, to generate improved wildfire smoke estimates, we construct an additional XGBoost-based ML model to predict wildfire smoke $PM_{2.5}$ estimates at all monitor locations that uses outputs from all three modeling approaches (Figure 1C):

$$PM_{smoke}^{monitor} = g(PM_{smoke}^{GC}, PM_{smoke}^{CMAQ}, PM_{smoke}^{ML}, ...) \text{ — trained on all days} \tag{2}$$

For each monitor-day, we first calculate wildfire smoke $PM_{2.5}$ ($PM_{smoke}^{monitor}$) as the difference between total $PM_{2.5}$ measurements and the constructed non-smoke $PM_{2.5}$ (estimated using equation 1). Our constructed non-smoke estimates better characterize the variability in daily non-smoke $PM_{2.5}$ relative to the constant non-smoke $PM_{2.5}$ baselines used in prior research (*9*). Furthermore, our estimates of smoke $PM_{2.5}$ at the monitor level do not depend on the HMS smoke plume boundaries, which are found to have large uncertainty under low and medium smoke conditions (*67*).

Separate calibration models are trained for the western US and the eastern US. The input features include smoke $PM_{2.5}$ estimated by GEOS-Chem, CMAQ, and ML, aerosol optical thickness from MERRA-2, meteorological variables including temperature, precipitation, wind speed, dew point temperature, planet boundary layer height, surface pressure, latitude, longitude, and day-of-year from ERA5. As our main purpose is to estimate wildfire smoke $PM_{2.5}$ for locations that are not covered by surface monitors, we evaluate the model performance using 5-fold spatial cross-validation. The spatial folds are defined considering the coarsest resolution of input features (in our case, the MERRA-2 inputs at 0.5 ° latitude × 0.625° longitude). Splitting train and test data sets by monitor locations rather than the more conventional method of random splitting by observation (in which a given monitor can contribute data to both train and test) is a more realistic evaluation of model performance as it avoids leakage of information between training and test sets. To measure variable importance in the XGBoost model, we use the contribution to model performance improvements from "tree splits" made on each feature.

Estimating dose-response function between mortality and wildfire smoke

We empirically estimate a dose-response function between smoke $PM_{2.5}$ and all-cause mortality rates using 2006-2020 county-level data (Figure 1D). As we only have CTM outputs in the year 2020, we construct four panels that include wildfire smoke from different estimation methods in 2020 (calibrated, GEOS-Chem, CMAQ, and ML), but the same wildfire smoke $PM_{2.5}$ estimates in 2006-2019 from the ML method (*9*). Therefore, our approach tests how a one-year difference in the wildfire smoke estimates influences the derived dose-response function.

Following a similar method in (*14*), we combine county-level population-weighted annual smoke $PM_{2.5}$, with county-level all-cause mortality rates by different age groups. We obtain individual-level multiple cause of death mortality data from the National Center for Health Statistics to calculate age-standardized mortality rates for all ages (*68*). County-level mortality rates were age-standardized using the direct method and 5-year bins (0-4, 5-9, ..., 85 and over) based on the 2000 US Census Standard Population. Monthly mortality rates were standardized per 100,000 people. To fully capture damages from ambient wildfire smoke concentrations, our preferred outcome is age-standardized, all-cause, all-age mortality rates at the county-year level.

In our main analysis, we estimate a Poisson model in which we allow non-linear impacts of annual smoke $PM_{2.5}$ on mortality rates at the county-year level following method from (*14*):

$$D_{csy} = \exp\,(\sum_i \beta_i smokeBIN^i_{csy} + \gamma W_{csy} + \eta_{sy} + \theta_c + \varepsilon_{csy}) \tag{3}$$

where D_{csy} denotes the age-adjusted all-cause mortality rates in county c, state s, and year y. $smokeBIN^i_{csy}$ is a dummy variable for whether annual population-weighted smoke $PM_{2.5}$ in county c, state s, and year y falls into the range of bin i (0-0.1, 0.1-0.25, 0.25-0.5, 0.5-0.75, 0.75-1, 1-2, 2-3, 3-4, 4-5, 5-6, >6 μg/m^3; 0-0.1 is the reference category). The main coefficients of interest are the β_i's, which estimate the effects of a year with annual smoke concentration of bin i on mortality rates, relative to a year with annual mean smoke $PM_{2.5}$ concentration below 0.1 μg/m^3. The reference category included <0.1 because only 4 county-year observations had exactly zero ambient wildfire smoke. W_{csy} denotes a flexible control of temperature (the number of days that fall in different temperature bins) and linear and quadratic terms of annual population-weighted precipitation. η_{sy} denotes a vector of state-year fixed effects (i.e. separate intercepts for each year in each state) that accounts for all factors that differ across states in a given year (e.g. California 2018 versus Oregon 2018) as well as all factors that differ within states across years (e.g. California 2017 versus California 2018). θ_c denotes a set of county-level fixed effects that accounts for any county-specific time-invariant factors that could be correlated with both smoke exposure and mortality. In essence, we identify the effect of wildfire smoke on mortality using within-county variation over time, after accounting for any factors that trend over time within that county's state, and for any correlation between smoke variation and variation in temperature and precipitation.

The coefficients are estimated using weighted Poisson regression models, with the function "fe-pois" from R package "fixest". The estimations are weighted by county-level population counts to enable estimates of population-averaged effects, as well as to reduce statistical uncertainty. The uncertainty of the coefficients is estimated using bootstrap of 500 runs. ϵ_{csy} represents the error terms.

Quantifying smoke-related health burdens

We quantify the excess mortality attributable to wildfire smoke in 2020, using the four different wildfire smoke estimates (from the three individual approaches and the calibrated model) and different dose-response functions. We first calculate the excess mortality using four empirically derived dose-response functions that are associated with each estimation method (as developed above). To understand the difference in health burdens associated with smoke $PM_{2.5}$ estimations alone, we further calculate the mortality burdens using the same dose-response functions applied to the wildfire smoke derived from different estimation methods. We use two dose-response functions, one at the annual level, and one at the daily level. At the annual level, we use the dose-response function derived using the wildfire smoke data from the ML method. At the daily level, we use the dose-response function from a recent meta-analysis (*19*). Meta-analyzing eight prior published estimates, Gould et al. estimated an increase in daily mortality rate by 0.15% (95% CI: 0.01%, 0.28%) per 1 $\mu g/m^3$ of smoke $PM_{2.5}$ on the same day (without considering lagged effects).

Results

Figure 2 shows the annual average wildfire smoke $PM_{2.5}$ concentration over the contiguous US (averaged from February-October in 2020) across the three estimation methods. We find that estimated wildfire smoke $PM_{2.5}$ concentrations vary substantially among the three approaches. In the western US, GEOS-Chem and CMAQ estimate much higher wildfire smoke concentrations compared to the ML estimates. For example, in Oregon and northern California, GEOS-Chem estimates an annual average smoke $PM_{2.5}$ concentration of >50 $\mu g/m^3$, while the ML estimates are 15-25 $\mu g/m^3$. Population-weighted wildfire smoke $PM_{2.5}$ exposure also differs dramatically. While all three methods estimate that the population-weighted average smoke $PM_{2.5}$ reaches the highest of the year on September 10-13, the max daily population-weighted mean smoke $PM_{2.5}$ estimated by GEOS-Chem (54.5 $\mu g/m^3$) is 3x the ML estimates (17.5 $\mu g/m^3$) and 2x the CMAQ estimates (25.4 $\mu g/m^3$). However, regional differences exist in the intercomparison of the three methods. In the southeastern US, CMAQ estimates are the highest among the three methods, and GEOS-Chem estimates are generally the lowest (Figure 2D). This could be due to the biased global Aerosol Optical Depth-based scaling factor used in the QFED emission inventory which results in higher estimated emissions in the southeast US (*31*, *69*).

The largest difference across three methods comes from their estimations of the smoke events in September 2020 in Oregon and California. When comparing model estimates over this region during a two-week period (September 6-20), we find even larger differences across methods (Figure 3). While the spatial distributions of wildfire smoke are similar across the three approaches, the estimated magnitude can differ by as much as 40x. The maximum daily smoke concentration for any grid cell in this region is estimated to be 32,700 $\mu g/m^3$ in GEOS-Chem, 17,300 $\mu g/m^3$ in CMAQ and 774 $\mu g/m^3$ in ML model. When comparing against surface measurements from EPA and PurpleAir sensors in this area, we find that the ML approach shows a much better agreement with surface measurements, while GEOS-Chem and CMAQ substantially overestimate surface $PM_{2.5}$ concentration (Figure 3D and 3E). The maximum daily smoke $PM_{2.5}$ concentration measured by any EPA or PurpleAir sensors is 821 $\mu g/m^3$ over this two-week period. We further investigate the significant model bias of the CTMs over this period, by conducting sensitivity simulations with varying injection heights and an alternative emission inventory in GEOS-Chem. We find the upward model bias in our original GEOS-Chem simulation (with default injection height and GFED emissions) is likely due to both the unrealistic injection heights and overestimated emissions in GFED, with the emissions being the more important factor (Figure S1).

Given the underlying uncertainty in the inferred monitor-level smoke $PM_{2.5}$, we further evaluate the performance of GEOS-Chem and CMAQ against surface measurements of total $PM_{2.5}$ (Figure 4 and S2). When there is no or low wildfire smoke, we find that CTMs can capture the overall spatial and temporal variability of $PM_{2.5}$ (Figure 4A). CTMs are generally able to predict the

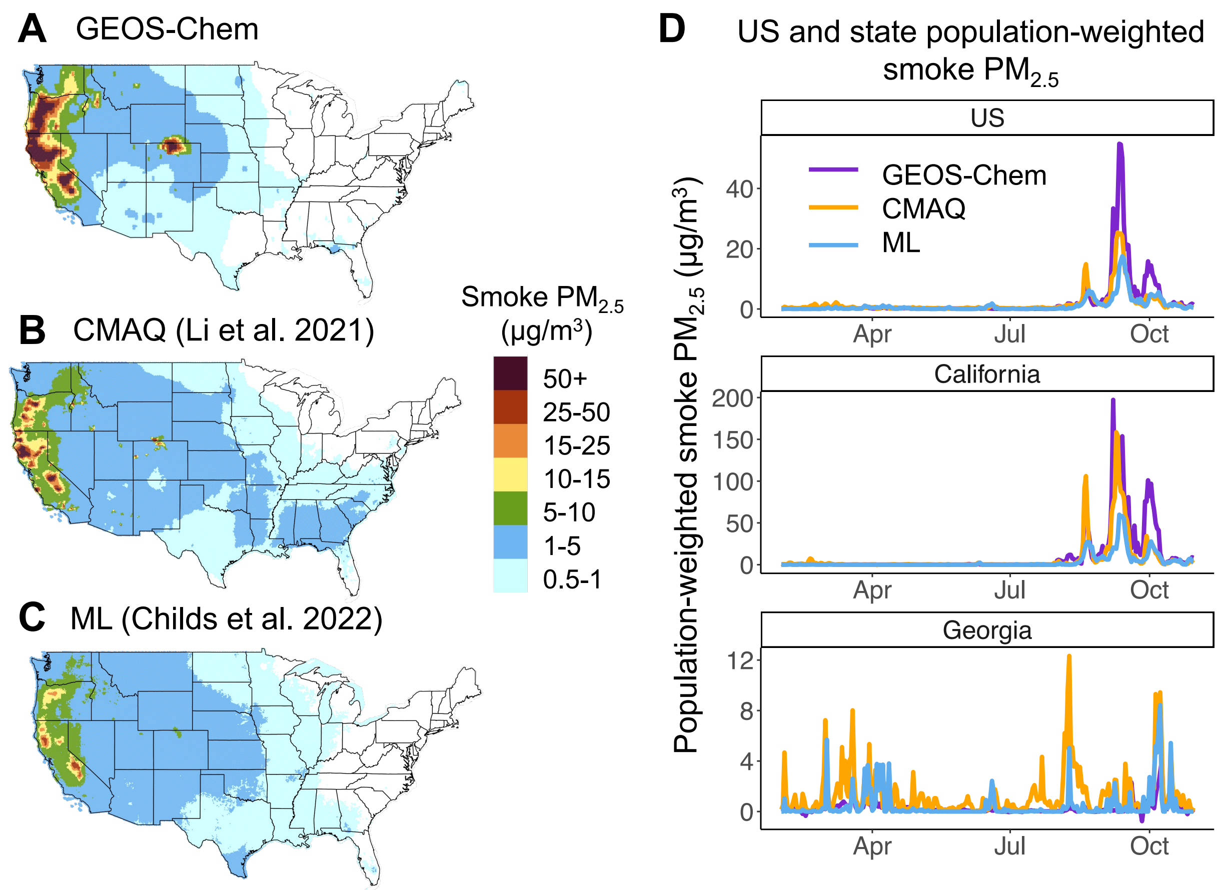

Figure 2: **Average smoke $PM_{2.5}$ concentration estimated by the three methods.** Panels A-C show the average smoke $PM_{2.5}$ concentration during February to October in 2020 estimated by GEOS-Chem (**A**), CMAQ (**B**, derived from (*11*)), and a ML method (**C**, derived from (*9*)). Panel D shows the population-weighted smoke $PM_{2.5}$ concentration in the contiguous US, California, and Georgia in 2020.

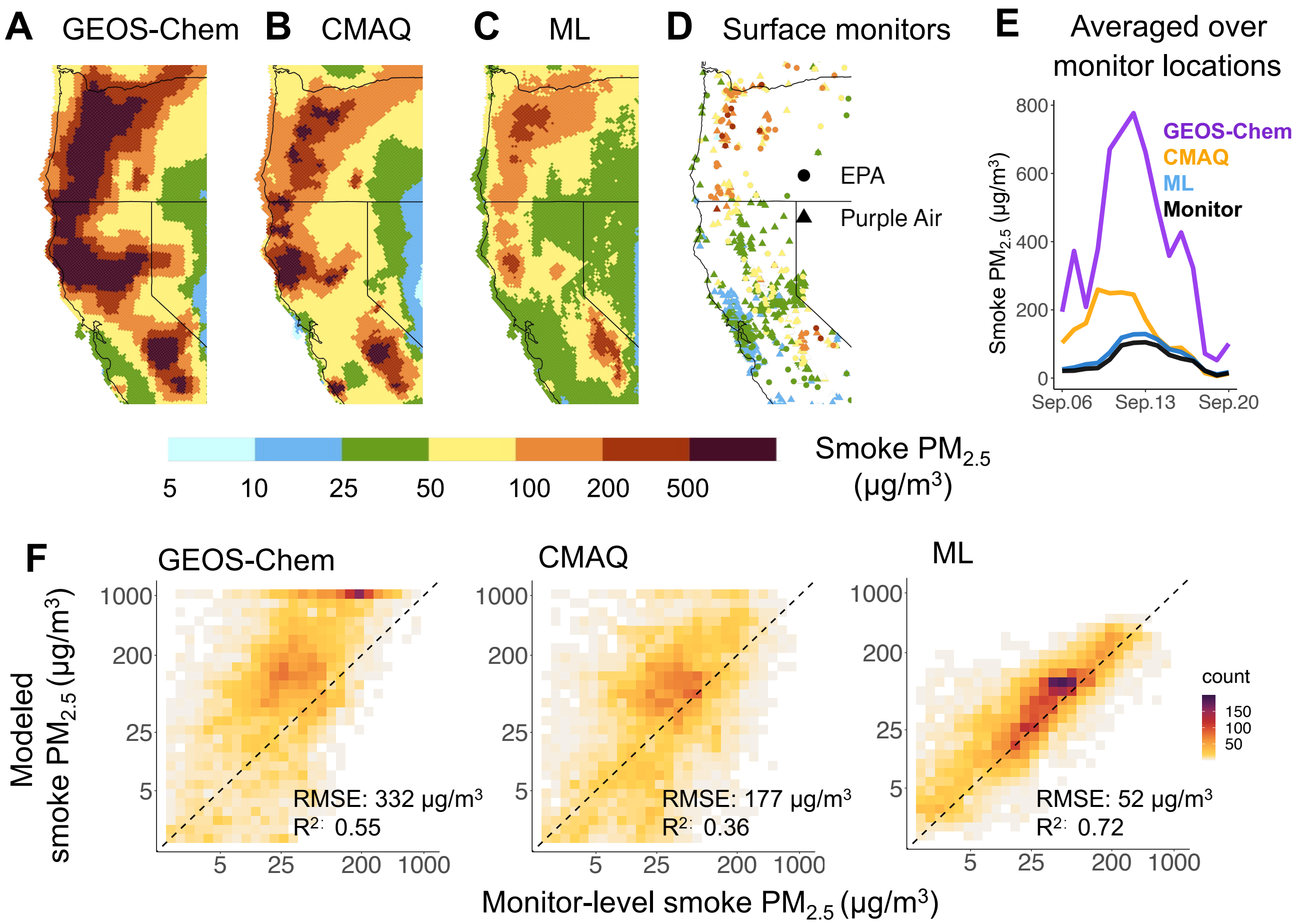

Figure 3: **Smoke $PM_{2.5}$ concentrations in extreme wildfire episodes in Oregon and northern California in September 2020.** Panels A-C show the average smoke $PM_{2.5}$ concentrations during September 6–20 estimated by GEOS-Chem, CMAQ, and ML, respectively. Panel D shows the average smoke $PM_{2.5}$ estimates derived from surface measurements of surface reference-grade monitors administered by US EPA and PurpleAir sensors. Panel E shows the average smoke $PM_{2.5}$ concentration estimated by different methods over all monitor locations. Panel F shows the estimated wildfire smoke $PM_{2.5}$ (y-axis) against the inferred smoke $PM_{2.5}$ at the monitor level. Inferred wildfire smoke $PM_{2.5}$ is estimated as the anomalous increases in total $PM_{2.5}$ when there is wildfire smoke overhead relative to baselines of $PM_{2.5}$ on non-smoke days, using a similar method as in Childs et al., 2022.

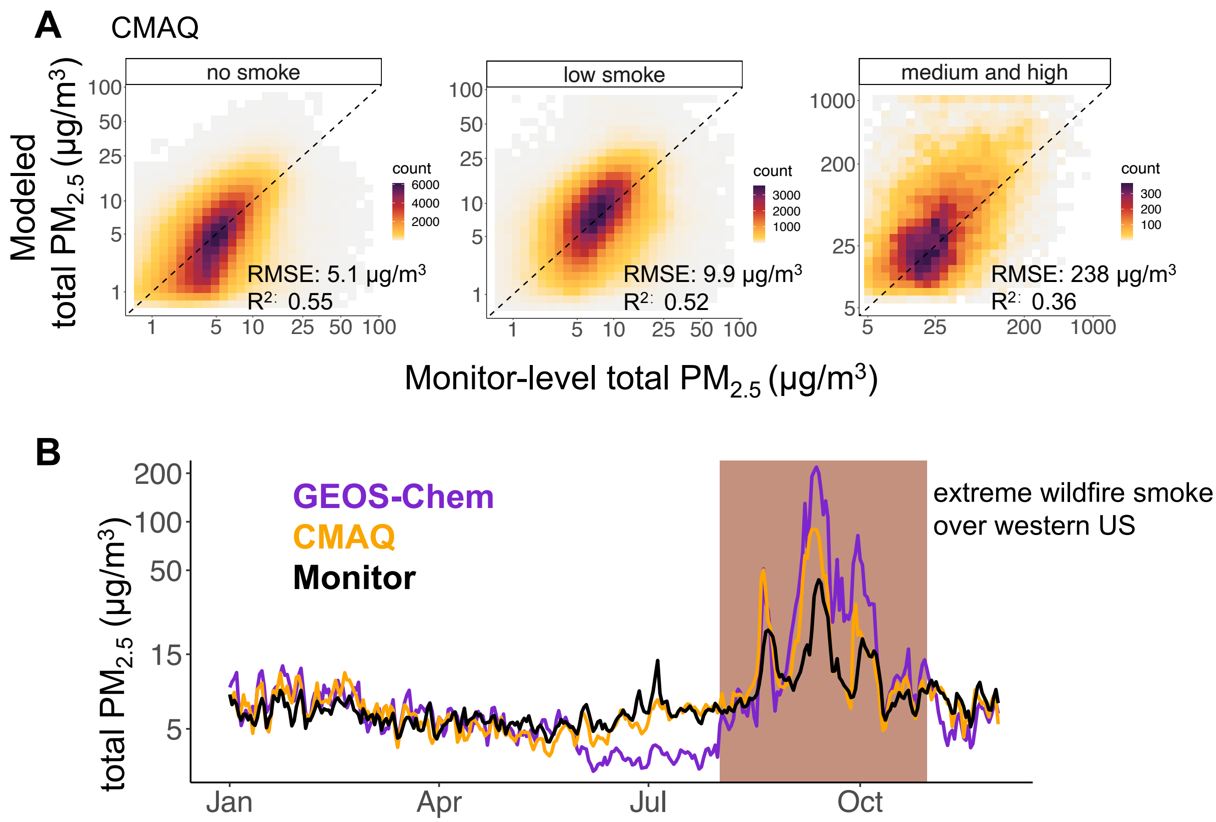

Figure 4: **Comparing CTM simulations of total $PM_{2.5}$ against surface measurements of total $PM_{2.5}$.** Panel A shows the total $PM_{2.5}$ concentration simulated by CMAQ (y-axis) against total $PM_{2.5}$ measurements from surface monitors under different levels of wildfire smoke. "No smoke" includes all monitor days with no smoke plume overhead and low estimated smoke concentrations from both CTM ($<0.5\ \mu g/m^3$). "Medium and high smoke" includes monitor-days with high estimated smoke $PM_{2.5}$ from both CTMs ($>5\ \mu g/m^3$). "Low smoke" category includes all the other conditions. Panel B shows the average total $PM_{2.5}$ concentration across all monitor locations in the US. The shade denotes a period when the western US experienced extreme wildfire smoke. Note the non-linear scale of y-axis for better visualization.

overall variability of $PM_{2.5}$ (Figure 4B), with the exception that the GEOS-Chem simulation shows a substantial downward bias in June and July, possibly due to over-partition of inorganic $PM_{2.5}$ species in the gas phase as suggested by (*70*) (see Figure S3). However, when there are medium and high levels of smoke in the air (defined by location-days that all three approaches agree that there is some smoke), we observe substantially larger differences between model simulations and surface measurements of total $PM_{2.5}$. The average $PM_{2.5}$ concentration simulated by GEOS-Chem and CMAQ is 5x and 3x the $PM_{2.5}$ concentrations measured by surface monitors, over all monitor locations and high smoke days.

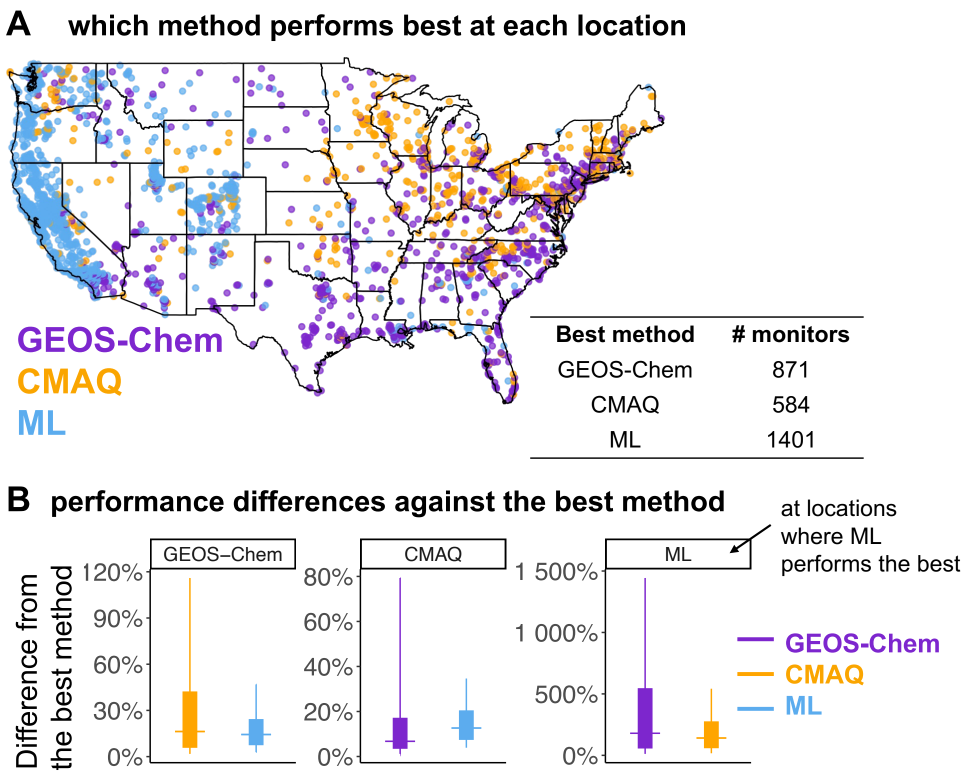

Figure 5: **Evaluating the performance of three wildfire smoke estimation methods against total $PM_{2.5}$ measurements from surface monitors.** Panel A shows the optimal estimation approach for each surface monitor location in our study. The color of the dots shows the optimal method at each location with the smallest RMSE against total $PM_{2.5}$ measurements. Table A shows the number of monitor locations that correspond to each of the estimation method. Panel B shows the difference in model performance from the best approach. For each panel, the bars show the range of performance difference against the best estimation approach (as shown in the panel title). The performance difference is measured as the relative difference between RMSE and RMSE of the best method. The solid bar shows the 25th and 75th percentile, and the line shows the median, 10th, and 90th percentile of the relative differences.

Using total $PM_{2.5}$ measurements from surface monitors as the evaluation benchmark, we identify the estimation approach with the best performance of characterizing smoke $PM_{2.5}$ in each monitor location in the US (Figure 5). We find that the ML approach performs the best in characterizing $PM_{2.5}$ concentrations in the western US where CTMs show a large model bias. However, GEOS-Chem and CMAQ outperform the ML approach in the eastern US, where low and medium levels of smoke are more prevalent. CTMs outperform the ML approach in these areas, possibly due to the uncertainty in non-smoke baselines used in the ML algorithm and the uncertainty of HMS smoke plumes over low and medium smoke conditions outside of the western US (*67*). As shown

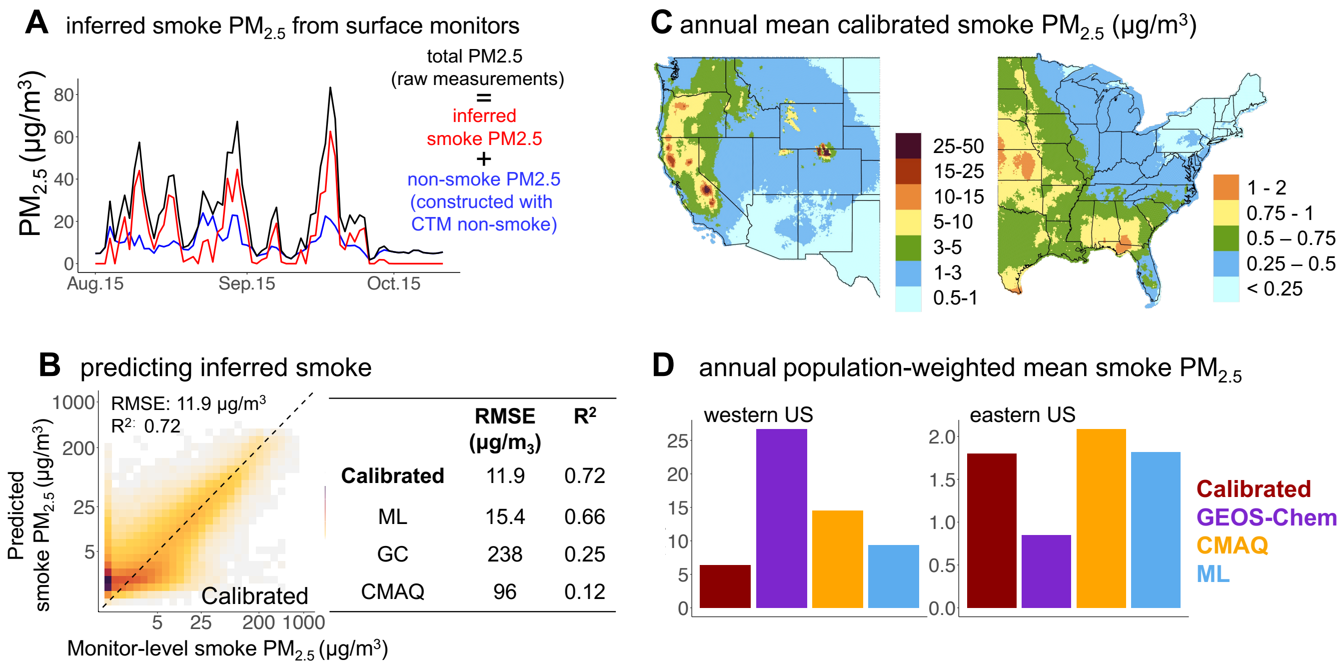

Figure 6: **Creating calibrated smoke $PM_{2.5}$ estimates using three individual smoke estimates.** Panel A shows how we infer smoke $PM_{2.5}$ from surface measurements. The inferred smoke $PM_{2.5}$ (shown in red) is calculated as the difference between the total $PM_{2.5}$ measurements (shown in black) and the non-smoke $PM_{2.5}$ constructed with non-smoke $PM_{2.5}$ estimates from CTMs and other co-variates (shown in blue). Panel B shows the performance of our calibration model. We use an XGBoost model to predict the inferred smoke $PM_{2.5}$ at the monitor level using the three wildfire smoke estimates and other features. The performance of the calibrated model is evaluated using a spatial 5-fold CV. Panel C shows the annual mean calibrated smoke $PM_{2.5}$ concentrations (from Feb-Oct). Note the different scales in the western and eastern US. Panel D shows the annual population-weighted mean smoke $PM_{2.5}$ estimates using the calibrated model and three individual estimates.

in Figure 5B, we find that in the locations where the ML method performs the best, ML methods significantly outperform CTM approaches (RMSE of CTM approach is 200-500% higher than the ML method). In the locations where CTM methods perform better, the relative gain in RMSE is smaller yet meaningful due to overall lower levels of smoke concentrations.

Integrating the three wildfire smoke estimates, we construct improved estimates of wildfire smoke $PM_{2.5}$ (referred to as "calibrated smoke $PM_{2.5}$" thereafter) constrained by surface measurements of total $PM_{2.5}$ and constructed non-smoke $PM_{2.5}$ concentrations (see Figure 6). The calibrated smoke $PM_{2.5}$ shows a better agreement with the inferred smoke $PM_{2.5}$ from surface monitors compared to the three individual approaches both over the entire study period (Figure 6B and S4) and during extreme smoke episodes (Table S1 and Figure S5). Consistent with the spatial pattern shown in

Figure 5A, we find that "ML smoke estimate" is the most important feature in the calibration model in the western US while all three estimates contribute to the calibration model in the eastern US (see Figure S6 for feature importance metrics). After calibration, we calculate that the annual average population-weighted smoke $PM_{2.5}$ concentration is 6.4 μg/m^3 in the western US in 2020, lower than all individual estimates. The calibrated estimates are even lower than ML estimates (7.7 μg/m^3) possibly because the calibrated model is also trained to predict measurements from PurpleAir sensors which are often placed in less polluted areas. In the eastern US, the calibrated model estimates an annual average population-weighted smoke $PM_{2.5}$ concentration of 1.8 μg/m^3 , which is in the range of the three individual estimates.

The different smoke $PM_{2.5}$ estimates (the three individual approaches and the calibrated) have important implications for empirically estimating dose-response function between smoke and all-cause mortality (Figure 7A), as well as the estimated mortality burden (Figure 7B). Even replacing one year of smoke data from different sources, we find important differences in the empirically estimated dose-response functions. While all dose-response functions show similar effects of smoke on mortality rates at lower annual smoke concentrations (e.g., below 0.5 μg/m^3), the effects can be quite different for extreme smoke exposure. This is because 2020 contributes to more observations in the high smoke bin compared to the low smoke bins. We estimate that years with extreme ambient wildfire smoke concentrations ($>$6 μg/m^3) increase annual mortality rates by 4.0% (95%CI: 1.0%, 7.4%) when using the calibrated smoke concentrations. The point estimate is smaller than point estimates derived from using ML (5.4%) or CMAQ smoke estimates (6.6%). However, if we use GEOS-Chem smoke estimates in 2020, we would find a negative (but statistically not significant) association between high annual smoke $PM_{2.5}$ concentration and mortality rates.

The different dose-response functions and estimated wildfire smoke exposures generate different estimates of excess deaths attributable to smoke $PM_{2.5}$ exposure in 2020, though the estimates are at comparable magnitudes (ranging from 18,200 to 43,957). When using different dose-response functions, the differences in estimated mortality can be as much as 2x across methods. The differences are smaller when using the same dose-response function, likely due to the fact that dose-response functions are estimated with binned smoke exposures and thus we treat all years with annual mean smoke above 6 μg/m^3 as the same. When using a linear dose-response function (which is used to estimate same-day mortalities), the differences across methods can be as much as 3x driven by the differences in estimated smoke concentrations.

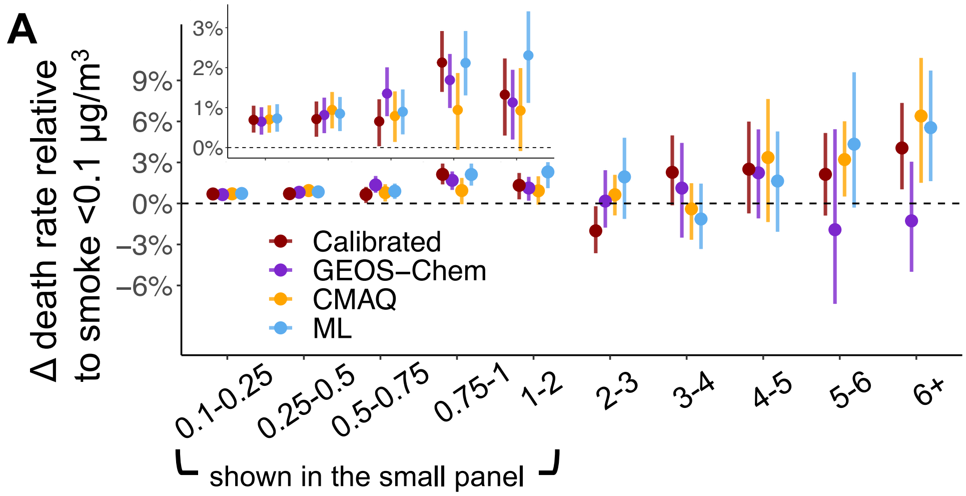

B

Outcome	Model	Mortality estimates		
Annual deaths	CMAQ	35,588	(13,166	56,439)
Different DRFs	GEOS-Chem	18,200	(2,456	33,300)
	ML	32,292	(17,498	46,865)
	Calibrated	23,224	(10,316	36,897)
Annual deaths	CMAQ	43,957	(25,551	61,991)
Same DRF (from ML)	GEOS-Chem	31,628	(16,107	47,672)
	ML	32,292	(17,498	46,865)
	Calibrated	30,330	(16,724	44,075)
Daily short-term deaths	CMAQ	5,296	(353	9,886)
DRF from Gould et al., 2023	GEOS-Chem	7,375	(492	13,767)
	ML	3,283	(219	6,128)
	Calibrated	2,818	(188	5,261)

Figure 7: **Empirically estimated impacts of wildfire smoke $PM_{2.5}$ on all-cause mortality rates and attributed mortality burden across different smoke estimates.** Panel A shows the effects of exposure to different annual mean concentration of smoke $PM_{2.5}$ (shown in the x-axis) relative to a year with smoke concentration <0.1 $\mu g/m^3$, estimated using a Poisson model at the county and annual level using data from 2006–2020. The wildfire smoke data is the same across estimations in 2006–2019 (derived from the ML method), but is different in 2020 depending on the estimation approach. Panel B shows the estimated excess deaths due to smoke $PM_{2.5}$ in 2020 using different dose-response functions (DRF) and smoke $PM_{2.5}$ estimated by different methods. "annual deaths, different DRF" is estimated using the DRFs shown in panel A. "annual deaths, same CRF" is estimated using the same DRF (derived from ML estimates) but different exposure estimates from the four methods. Thus, the difference is only due to different estimates of wildfire smoke $PM_{2.5}$ concentration. "daily short-term deaths" is estimated using the same DRF across four estimations methods by using the DRF from (*19*), which estimates the effects of daily wildfire smoke $PM_{2.5}$ on same-day mortality rates. The error bars and values in the parenthesis show the 95% confidence interval estimated using bootstrapping.

Discussion

We find substantial discrepancies in estimated wildfire smoke $PM_{2.5}$ concentrations across three widely-used approaches in the US during 2020, the most extreme smoke year in the recent history of the US but likely to be more prevalent under future climate change. Therefore, our results have implications for estimating future fire smoke exposure and health impacts. Among the three approaches we evaluate, we find that the ML approach performs better in the western US with high-level of smoke, while CTM approaches exhibit large biases due to biased emissions inventory and incorrectly-modeled injection heights. On the other hand, CTM approaches outperform the ML approach in the eastern US, due to the uncertainty of the underlying smoke plume data and the calculated non-smoke baselines used in the ML approach. To address the discrepancies across methods, we develop a calibration approach that uses all three wildfire smoke estimates to generate improved estimates of wildfire smoke that better match surface measurements of air quality. Given the improved performance against surface measurement throughout the US, our improved estimates of smoke $PM_{2.5}$ are appropriate for downstream health impacts analysis.

Consistent with the large literature on environmental health and epidemiology, our research demonstrates that the measurement of environmental exposures matters for estimating downstream health impacts. Perhaps surprisingly, we find that only one year of different exposures in our 15 years of data can generate large differences in the estimated dose-response function. In our case, incorrect exposures can lead to suspicious associations between wildfire smoke and mortality (e.g., GEOS-Chem model results show negative associations between extreme wildfire smoke and mortality rates). Therefore, one important message our work has for health researchers is to use non-validated exposure metrics with extreme caution, and to validate/calibrate them against in-situ measurements before using them for estimating health impacts. We also show that the differences in exposure can lead to larger uncertainties in dose-response functions compared to estimates of health burdens. This occurs because noisy yet unbiased exposure estimates can substantially attenuate estimates of the dose-response function, effectively biasing down the relationship. Conversely, applying a roughly linear dose-response function to various exposures may result in similar levels of health burdens, as noise in the exposure data cancels out. Given the widespread use of empirically-estimated dose-response functions, our research demonstrates the importance of correctly modelling smoke pollution exposure in the first place, and how calibrations of the model estimates can improve the downstream health impact analysis.

Despite the uncertainty in wildfire smoke estimates, we find that increasing annual exposures to smoke $PM_{2.5}$ are associated with higher county-level annual mortality rates across the contiguous US. Using our calibrated smoke estimates, we estimate more than 23,000 deaths attributable to exposure to wildfire smoke in 2020. Our work contributes to a large and growing body of literature documenting the impacts of annual exposures to total $PM_{2.5}$ on mortality, which has shaped decades of policy to improve ambient air quality in the US. However, wildfires are episodic and typically generate short-term spikes in ambient air pollution (*71*). In a sensitivity analysis, we show that using short-term daily extremes (i.e., the number of extreme smoke days in a year) to estimate mortality yields similar (but more noisy) estimates to our main estimates using annual average smoke exposure (see Figure S7), likely because annual changes in exposure are driven substantially by increases in short-run extremes. We observe similar discrepancies in the derived dose-response functions that link the number of extreme smoke days to annual mortality across the smoke estimation methods.

Our research points to several potential areas for future research to improve our understanding of the health effects of wildfire smoke. A more in-depth comparison based on multiple years of wildfire smoke estimates will help understand the generalizability of our findings and evaluate the influences of smoke estimation methods on health effects beyond 2020. While our research selects three widely-used wildfire smoke estimation methods, we do not fully explore the whole suite of wildfire smoke estimation approaches, such as other CTMs using different emission inventories and injection heights and alternate ML algorithms. Nevertheless, our framework of evaluation and calibration of wildfire smoke estimates can be extended to other wildfire estimates generated by other CTMs or data-driven techniques. Due to the limited temporal resolution of the mortality data, we demonstrate the influence of wildfire smoke estimates on the annual smoke-mortality relationship. Given the established short-term effects of wildfire smoke on health outcomes (*19*), future research can evaluate how different wildfire smoke estimates can influence short-term health dose-response functions.

Acknowledgments

We thank Yunyao Li, Marissa Childs, and Jessica Li for sharing smoke $PM_{2.5}$ estimates. We thank members of Stanford Environmental Change and Human Outcome Lab and Center on Food Security and the Environment for helpful comments. MQ acknowledges the support from the planetary health fellowship at Stanford's Center for Innovation in Global Health. DT acknowledges the support from NASA Health and Air Quality Program and contributions from members in GMU air quality team. Some of the computing for this project was performed on the Stanford Sherlock cluster, and we would like to thank Stanford University and the Stanford Research Computing Center for providing computational resources and support that contributed to these research results.

Author contributions

MQ and MB designed the study. MK and XJ performed the GEOS-Chem model simulations. DT provided the CMAQ simulation. SHN collected and calibrated the PurpleAir data. MQ led the evaluation of the smoke products and health impacts analysis, with input from all co-authors. MQ and MB drafted the manuscript with input from all co-authors. All authors contributed to interpretation of results and reviewed the manuscript.

Competing interests

The authors declare no competing interests.

Data and materials availability

Data and code to replicate all results in the main text and supplementary materials will be made available at a public repository, except for county-level mortality data for low-population counties, which are not publicly available and were obtained through application to the National Center for Health Statistics.

References

1. V. Iglesias, J. K. Balch, W. R. Travis, US fires became larger, more frequent, and more widespread in the 2000s. *Science advances* **8**, eabc0020 (2022).

2. J. T. Abatzoglou, A. P. Williams, Impact of anthropogenic climate change on wildfire across western US forests. *Proceedings of the National Academy of Sciences* **113**, 11770–11775 (2016).

3. Y. Zhuang, R. Fu, B. D. Santer, R. E. Dickinson, A. Hall, Quantifying contributions of natural variability and anthropogenic forcings on increased fire weather risk over the western United States. *Proceedings of the National Academy of Sciences* **118**, e2111875118 (2021).

4. N. S. Diffenbaugh, A. G. Konings, C. B. Field, Atmospheric variability contributes to increasing wildfire weather but not as much as global warming. *Proceedings of the National Academy of Sciences* **118**, e2117876118 (2021).

5. Z. L. Steel, H. D. Safford, J. H. Viers, The fire frequency-severity relationship and the legacy of fire suppression in California forests. *Ecosphere* **6**, 1–23 (2015).

6. V. C. Radeloff *et al.*, Rising wildfire risk to houses in the United States, especially in grasslands and shrublands. *Science* **382**, 702–707 (2023).

7. C. D. McClure, D. A. Jaffe, US particulate matter air quality improves except in wildfire-prone areas. *Proceedings of the National Academy of Sciences* **115**, 7901–7906 (2018).

8. K. O'Dell, B. Ford, E. V. Fischer, J. R. Pierce, Contribution of wildland-fire smoke to US PM2. 5 and its influence on recent trends. *Environmental science & technology* **53**, 1797–1804 (2019).

9. M. L. Childs *et al.*, Daily Local-Level Estimates of Ambient Wildfire Smoke PM2. 5 for the Contiguous US. *Environmental Science & Technology* **56**, 13607–13621 (2022).

10. D. Zhang *et al.*, Wildland Fires Worsened Population Exposure to PM2. 5 Pollution in the Contiguous United States. *Environmental Science & Technology* **57**, 19990–19998 (2023).

11. Y. Li *et al.*, Dominance of wildfires impact on air quality exceedances during the 2020 record-breaking wildfire season in the United States. *Geophysical Research Letters* **48**, e2021GL094908 (2021).

12. M. Burke *et al.*, The changing risk and burden of wildfire in the United States. *Proceedings of the National Academy of Sciences* **118**, e2011048118 (2021).

13. M. Burke *et al.*, The contribution of wildfire to PM2. 5 trends in the USA. *Nature* **622**, 761–766 (2023).

14. M. Qiu *et al.*, Wildfire smoke exposure and mortality burden in the US under future climate change. (2024).

15. B. Ford *et al.*, Future fire impacts on smoke concentrations, visibility, and health in the contiguous United States. *GeoHealth* **2**, 229–247 (2018).

16. J. C. Liu *et al.*, Future respiratory hospital admissions from wildfire smoke under climate change in the Western US. *Environmental Research Letters* **11**, 124018 (2016).

17. J. E. Neumann *et al.*, Estimating PM2. 5-related premature mortality and morbidity associated with future wildfire emissions in the western US. *Environmental Research Letters* **16**, 035019 (2021).

18. C. E. Reid *et al.*, Critical review of health impacts of wildfire smoke exposure. *Environmental health perspectives* **124**, 1334–1343 (2016).

19. C. F. Gould *et al.*, Health effects of wildfire smoke exposure. *Annual Review of Medicine* **75** (2023).

20. X. Ye *et al.*, Evaluation and intercomparison of wildfire smoke forecasts from multiple modeling systems for the 2019 Williams Flats fire. *Atmospheric Chemistry and Physics* **21**, 14427–14469 (2021).

21. P Makkaroon *et al.*, Development and evaluation of a North America ensemble wildfire air quality forecast: Initial application to the 2020 Western United States "Gigafire". *Journal of Geophysical Research: Atmospheres* **128**, e2022JD037298 (2023).

22. C. Black, Y. Tesfaigzi, J. A. Bassein, L. A. Miller, Wildfire smoke exposure and human health: Significant gaps in research for a growing public health issue. *Environmental toxicology and pharmacology* **55**, 186–195 (2017).

23. R. W. Gan *et al.*, Comparison of wildfire smoke estimation methods and associations with cardiopulmonary-related hospital admissions. *GeoHealth* **1**, 122–136 (2017).

24. V. A. Williams *et al.*, Impact of wildfires on cardiovascular health. *Circulation research* **134**, 1061–1082 (2024).

25. S. Rajagopalan, S. G. Al-Kindi, R. D. Brook, Air pollution and cardiovascular disease: JACC state-of-the-art review. *Journal of the American College of Cardiology* **72**, 2054–2070 (2018).

26. G. Chen *et al.*, Mortality risk attributable to wildfire-related PM2· 5 pollution: a global time series study in 749 locations. *The Lancet Planetary Health* **5**, e579–e587 (2021).

27. A. Heaney *et al.*, Impacts of fine particulate matter from wildfire smoke on respiratory and cardiovascular health in California. *GeoHealth* **6**, e2021GH000578 (2022).

28. T. Ye *et al.*, Short-term exposure to wildfire-related PM2. 5 increases mortality risks and burdens in Brazil. *Nature Communications* **13**, 7651 (2022).

29. S. Pan *et al.*, Quantifying the premature mortality and economic loss from wildfire-induced PM2. 5 in the contiguous US. *Science of The Total Environment* **875**, 162614 (2023).

30. Y.-Y. Meng *et al.*, Health and economic cost estimates of short-term total and wildfire PM2. 5 exposure on work loss: using the consecutive California Health Interview Survey (CHIS) data 2015–2018. *BMJ Public Health* **2** (2024).

31. X. Pan *et al.*, Six global biomass burning emission datasets: intercomparison and application in one global aerosol model. *Atmospheric Chemistry and Physics* **20**, 969–994 (2020).

32. T. S. Carter *et al.*, How emissions uncertainty influences the distribution and radiative impacts of smoke from fires in North America. *Atmospheric Chemistry and Physics* **20**, 2073–2097 (2020).

33. Y. Li *et al.*, Impacts of estimated plume rise on PM 2.5 exceedance prediction during extreme wildfire events: a comparison of three schemes (Briggs, Freitas, and Sofiev). *Atmospheric Chemistry and Physics* **23**, 3083–3101 (2023).

34. X. Huang *et al.*, Smoke-weather interaction affects extreme wildfires in diverse coastal regions. *Science* **379**, 457–461 (2023).

35. Y. Xie, M. Lin, L. W. Horowitz, Summer PM2. 5 pollution extremes caused by wildfires over the western United States during 2017–2018. *Geophysical Research Letters* **47**, e2020GL089429 (2020).

36. X. Feng *et al.*, Improved estimates of smoke exposure during Australia fire seasons: importance of quantifying plume injection heights. *Atmospheric Chemistry and Physics* **24**, 2985–3007 (2024).

37. J. C. Liu *et al.*, Wildfire-specific fine particulate matter and risk of hospital admissions in urban and rural counties. *Epidemiology* **28**, 77–85 (2017).

38. C. E. Reid, E. M. Considine, M. M. Maestas, G. Li, Daily PM2. 5 concentration estimates by county, ZIP code, and census tract in 11 western states 2008–2018. *Scientific data* **8**, 112 (2021).

39. W. Lassman *et al.*, Spatial and temporal estimates of population exposure to wildfire smoke during the Washington state 2012 wildfire season using blended model, satellite, and in situ data. *GeoHealth* **1**, 106–121 (2017).

40. G. Geng *et al.*, Satellite-based daily PM2. 5 estimates during fire seasons in Colorado. *Journal of Geophysical Research: Atmospheres* **123**, 8159–8171 (2018).

41. R. Aguilera *et al.*, A novel ensemble-based statistical approach to estimate daily wildfire-specific PM2. 5 in California (2006–2020). *Environment international* **171**, 107719 (2023).

42. Y. Ma *et al.*, Wildfire smoke PM2. 5 and mortality in the contiguous United States. *medRxiv* (2023).

43. S. Heft-Neal *et al.*, Emergency department visits respond nonlinearly to wildfire smoke. *Proceedings of the National Academy of Sciences* **120**, e2302409120 (2023).

44. C. Chen, L. Schwarz, N. Rosenthal, M. E. Marlier, T. Benmarhnia, Exploring spatial heterogeneity in synergistic effects of compound climate hazards: Extreme heat and wildfire smoke on cardiorespiratory hospitalizations in California. *Science Advances* **10**, eadj7264 (2024).

45. Q. Zhu *et al.*, Wildfires are associated with increased emergency department visits for anxiety disorders in the western United States. *Nature Mental Health*, 1–9 (2024).

46. A. L. Johnson, M. J. Abramson, M. Dennekamp, G. J. Williamson, Y. Guo, Particulate matter modelling techniques for epidemiological studies of open biomass fire smoke exposure: a review. *Air Quality, Atmosphere & Health* **13**, 35–75 (2020).

47. X. Jiang, E.-H. Enki Yoo, Modeling wildland fire-specific PM2. 5 concentrations for uncertainty-aware health impact assessments. *Environmental science & technology* **53**, 11828–11839 (2019).

48. W. Yuchi *et al.*, Blending forest fire smoke forecasts with observed data can improve their utility for public health applications. *Atmospheric Environment* **145**, 308–317 (2016).

49. E. M. Considine *et al.*, Evaluation of model-based PM2. 5 estimates for exposure assessment during wildfire smoke episodes in the western US. *Environmental Science & Technology* **57**, 2031–2041 (2023).

50. G. R. Van Der Werf *et al.*, Global fire emissions estimates during 1997–2016. *Earth System Science Data* **9**, 697–720 (2017).

51. I. Bey *et al.*, Global modeling of tropospheric chemistry with assimilated meteorology: Model description and evaluation. *Journal of Geophysical Research: Atmospheres* **106**, 23073–23095 (2001).

52. S. Akagi *et al.*, Emission factors for open and domestic biomass burning for use in atmospheric models. *Atmospheric Chemistry and Physics* **11**, 4039–4072 (2011).

53. M. Mu *et al.*, Daily and 3-hourly variability in global fire emissions and consequences for atmospheric model predictions of carbon monoxide. *Journal of Geophysical Research: Atmospheres* **116** (2011).

54. E. V. Fischer *et al.*, Atmospheric peroxyacetyl nitrate (PAN): a global budget and source attribution. English, *Atmospheric Chemistry and Physics* **14**, 2679 –2698 (2014).

55. J. W. Kaiser *et al.*, Biomass burning emissions estimated with a global fire assimilation system based on observed fire radiative power. English, *Biogeosciences* **9**, 527 –554 (2012).

56. S. Rémy *et al.*, Two global data sets of daily fire emission injection heights since 2003. *Atmospheric Chemistry and Physics* **17**, 2921–2942 (May 2017).

57. X Zhang *et al.*, *The blended global biomass burning emissions product from MODIS and VIIRS observations (GBBEPx) version 3.1*, 2019.

58. M Sofiev, T Ermakova, R Vankevich, Evaluation of the smoke-injection height from wild-land fires using remote-sensing data. *Atmospheric Chemistry and Physics* **12**, 1995–2006 (2012).

59. Y Li *et al.*, Ensemble PM2. 5 forecasting during the 2018 camp fire event using the HYSPLIT transport and dispersion model. *Journal of Geophysical Research: Atmospheres* **125**, e2020JD032768 (2020).

60. U.S. Environmental Protection Agency, *Air Data: Air Quality Data Collected at Outdoor Monitors Across the US*, 2023.

61. Jenny L. Hand, *IMPROVE DATA USER GUIDE 2023 (VERSION 2)*, 2023.

62. M. Burke *et al.*, Exposures and behavioural responses to wildfire smoke. *Nature human behaviour* **6**, 1351–1361 (2022).

63. D. A. Jaffe *et al.*, Wildfire and prescribed burning impacts on air quality in the United States. *Journal of the Air & Waste Management Association* **70**, 583–615 (2020).

64. K. K. Barkjohn, A. L. Holder, S. G. Frederick, A. L. Clements, Correction and accuracy of PurpleAir PM2. 5 measurements for extreme wildfire smoke. *Sensors* **22**, 9669 (2022).

65. W Schroeder *et al.*, Validation analyses of an operational fire monitoring product: The Hazard Mapping System. *International Journal of Remote Sensing* **29**, 6059–6066 (2008).

66. S. E. Cleland *et al.*, Estimating wildfire smoke concentrations during the October 2017 California fires through BME space/time data fusion of observed, modeled, and satellite-derived PM2. 5. *Environmental science & technology* **54**, 13439–13447 (2020).

67. T. Liu *et al.*, Is the smoke aloft? Caveats regarding the use of the Hazard Mapping System (HMS) smoke product as a proxy for surface smoke presence across the United States. (2023).

68. National Center for Health Statistics Division of Vital Statistics, *NVSS Restricted-use Mortality Files, 1999-2021. Hyattsville, Maryland.*

69. T. Liu *et al.*, Diagnosing spatial biases and uncertainties in global fire emissions inventories: Indonesia as regional case study. *Remote Sensing of Environment* **237**, 111557 (2020).

70. P. S. Kim *et al.*, Sources, seasonality, and trends of southeast US aerosol: an integrated analysis of surface, aircraft, and satellite observations with the GEOS-Chem chemical transport model. *Atmospheric Chemistry and Physics* **15**, 10411–10433 (2015).

71. J. A. Casey *et al.*, Measuring long-term exposure to wildfire PM2. 5 in California: Time-varying inequities in environmental burden. *Proceedings of the National Academy of Sciences* **121**, e2306729121 (2024).

Supplementary tables

Table S1: RMSE between the inferred smoke $PM_{2.5}$ at the monitor level and different fire smoke $PM_{2.5}$ estimates. The table compares the inferred smoke $PM_{2.5}$ concentrations with smoke estimated by two calibration models and three individual methods. "Calibration" is our main calibration model that uses all surface measurements, and "Calibration-extreme" up-weights the extreme smoke days for a better representation of the extreme conditions in the calibration process. The table shows the results for the western US and eastern US, respectively, and for extreme and non-extreme smoke conditions. Extreme smoke day are defined as days with smoke $PM_{2.5}$ over 50 $\mu g/m^3$ in the western US or 15 $\mu g/m^3$ in the eastern US. The RMSE is calculated with spatial 5-fold CV for the calibration models.

	Western US (longitude < -100)		Eastern US (longitude > -100)	
	non-extreme	extreme	non-extreme	extreme
Calibration	7.3	64	2.2	37
Calibration-extreme	11	61	5.3	35
GEOS-Chem	140	1313	2.7	38
CMAQ	81	445	3.3	37
ML	12	73	3.0	37

Supplementary figures

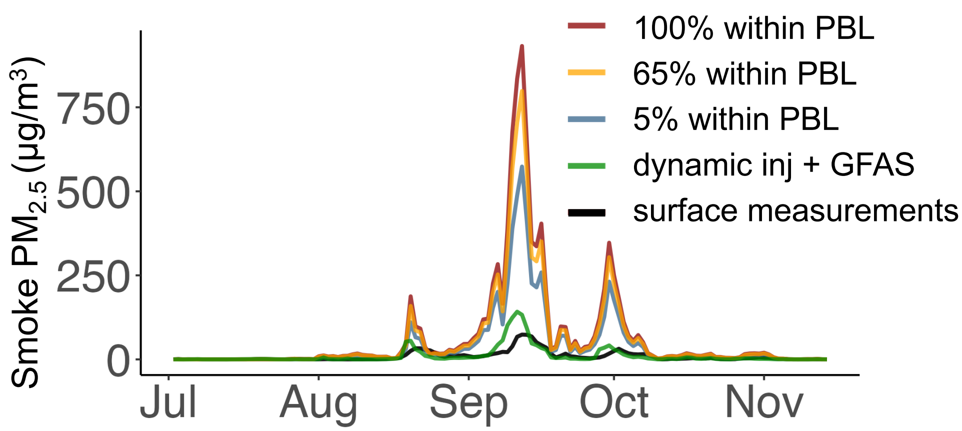

Figure S1: Estimated wildfire smoke $PM_{2.5}$ in Oregon and California by GEOS-Chem, under alternate injection heights and emission inventories. The plot shows the daily smoke $PM_{2.5}$ concentrations averaged over all monitor locations in Oregon and California. The black line shows the smoke $PM_{2.5}$ derived from surface measurements. In the main analysis, our GEOS-Chem simulation uses GFED4s emission inventory and assumes 100% of the emission occurred within Planetary Boundary Layer. The plot shows the simulations from three sensitivity scenarios: GFED4s emissions with alternative injection heights (65% or 5% emissions occurred within PBL), and a scenario using dynamic injection height and GFAS emission inventory (see Method).

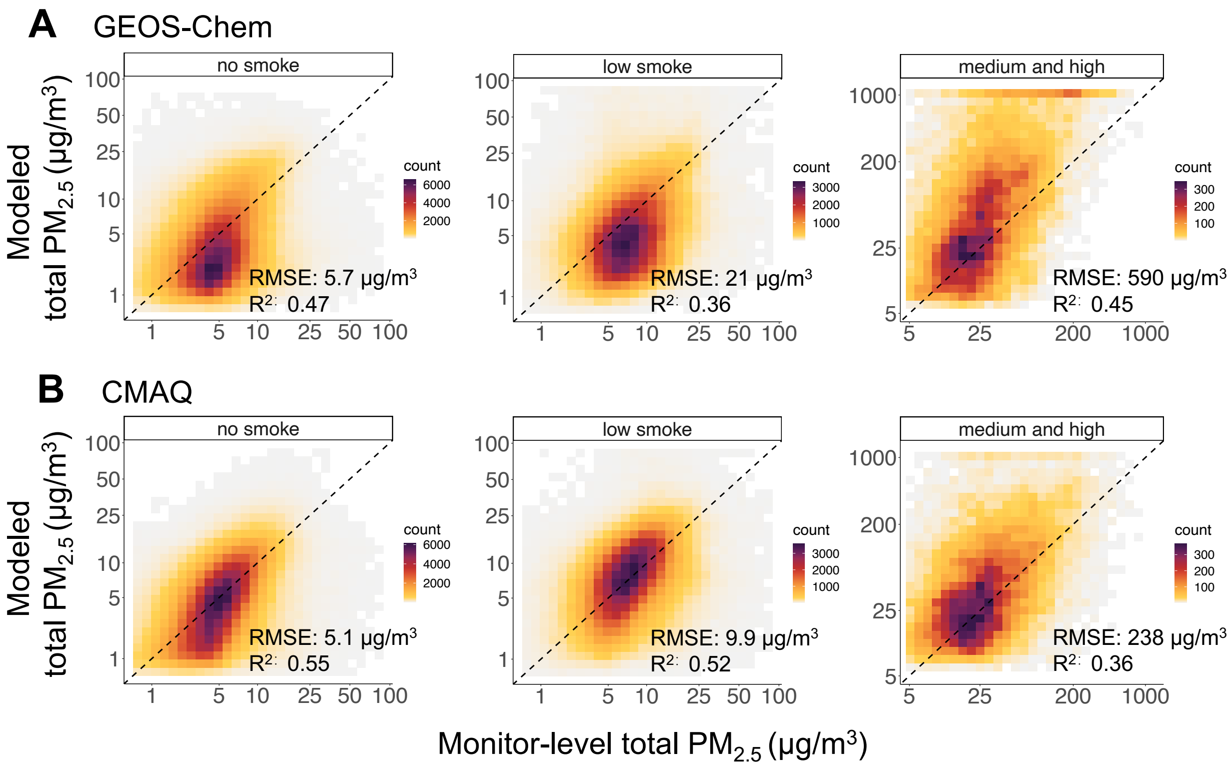

Figure S2: Simulated total $PM_{2.5}$ concentrations compared against surface measurements across different smoke conditions. "No smoke" includes all monitor days with no smoke plume overhead and low estimated smoke concentrations from both CTM (<0.5 $\mu g/m^3$). "Medium and high smoke" includes monitor days with high estimated smoke $PM_{2.5}$ from both CTMs (>5 $\mu g/m^3$). "Low smoke" category includes all the other conditions.

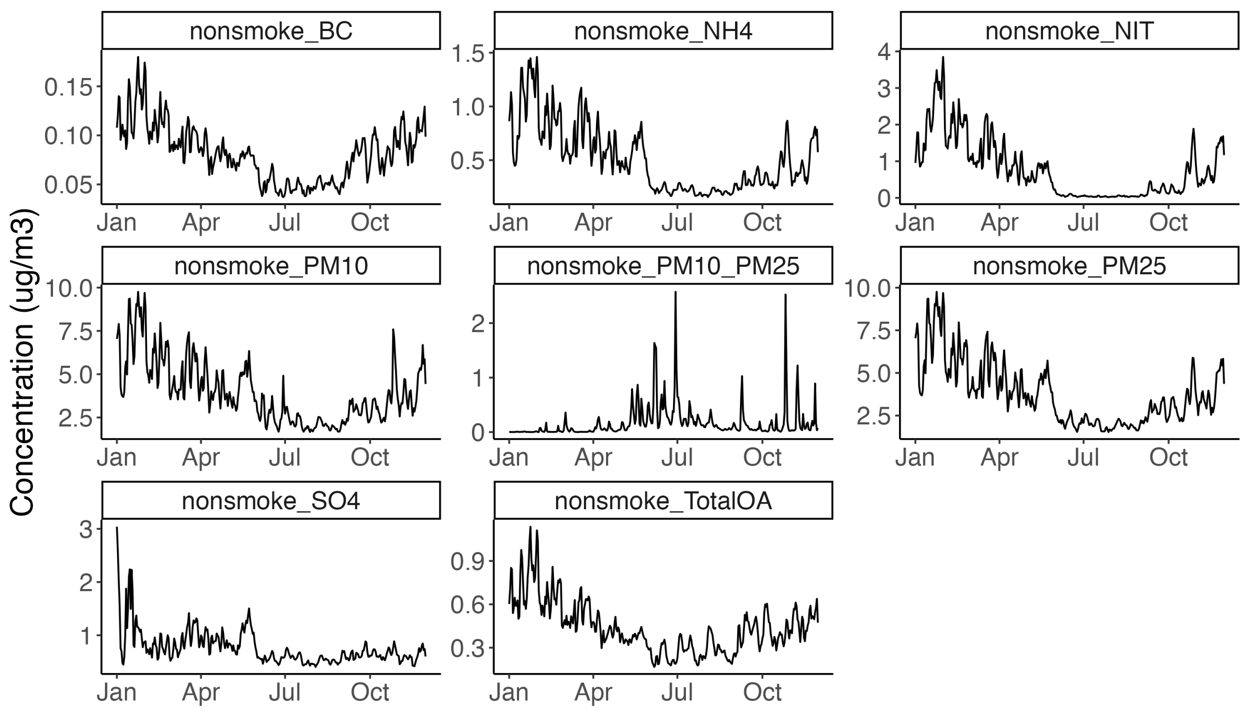

Figure S3: Concentrations of $PM_{2.5}$ components, PM_{10}, and coarse PM (PM_{10} - $PM_{2.5}$) simulated by GEOS-Chem under the no-wildfire scenario. The plot shows the concentration averaged over all US monitor location for black carbon (BC), ammonium (NH4), nitrate (NIT), PM_{10}, coarse PM (PM_{10} - $PM_{2.5}$), $PM_{2.5}$, sulfate (SO_4), and total organic aerosol (TotalOA).

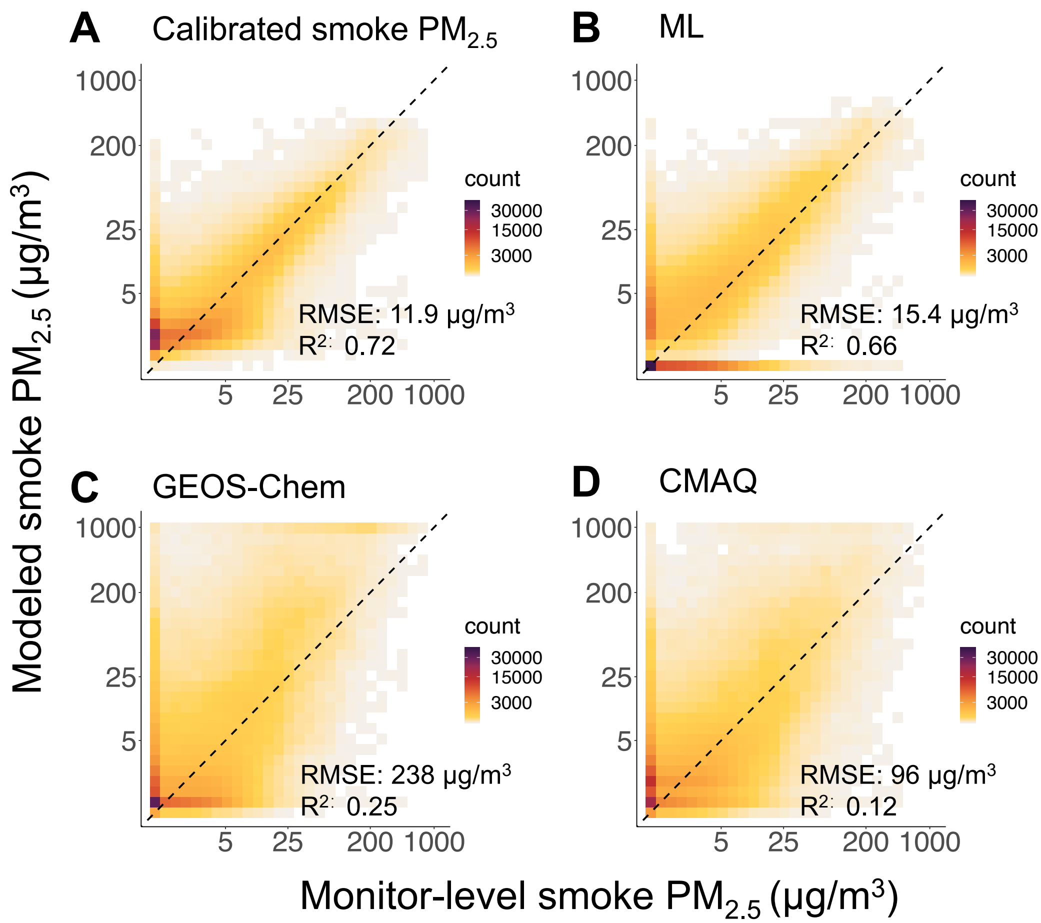

Figure S4: Estimated smoke $PM_{2.5}$ (y-axis) compared against the inferred smoke $PM_{2.5}$ concentrations at the surface monitors (x-axis). Panel A shows the calibrated smoke $PM_{2.5}$ derived from the machine learning model that uses three individual smoke $PM_{2.5}$ simulated by CTMs to predict surface $PM_{2.5}$ under smoke days. Panel B-D show the non-smoke $PM_{2.5}$ concentrations simulated by ML, GEOS-Chem, and CMAQ.

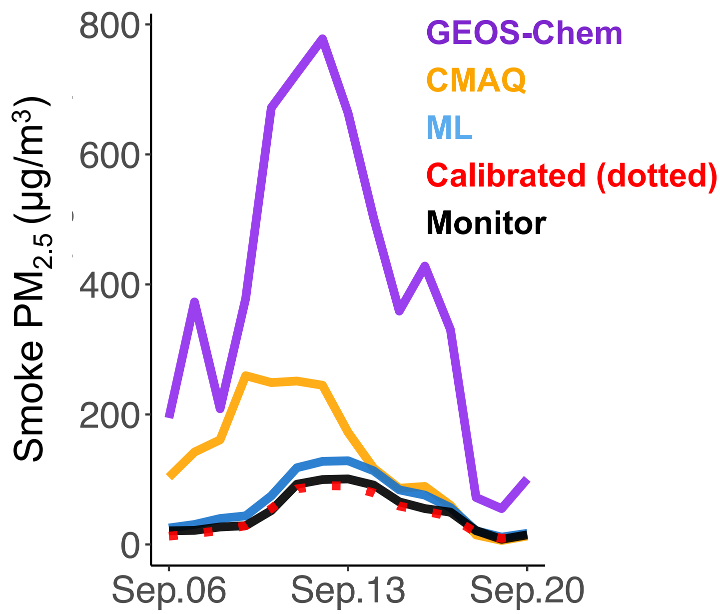

Figure S5: The plot shows the average smoke $PM_{2.5}$ concentrations estimated by different methods over all monitor locations in the western US during September 2020. The spatial range of the monitors is shown in Figure 3.

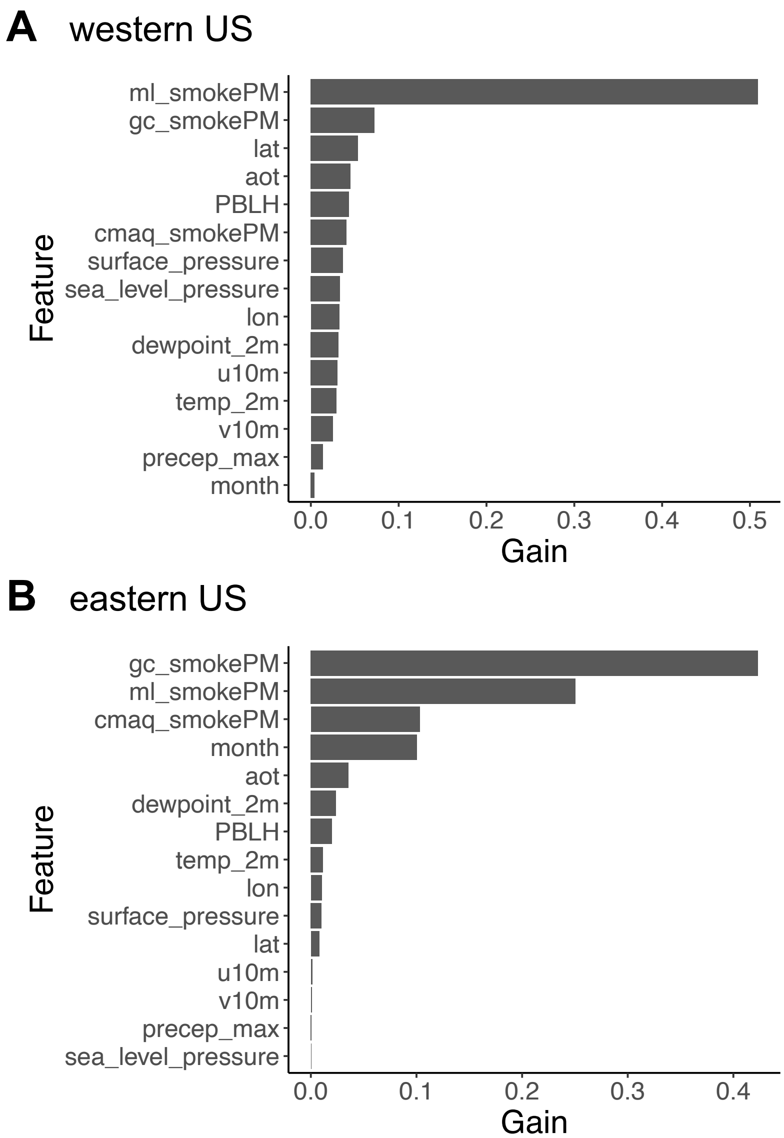

Figure S6: Feature importance of the XGBoost model to calibrate the smoke $PM_{2.5}$ estimates in the western US (Panel A) and the eastern US (Panel B). The y-axis shows the normalized gain of each feature in the model, defined as the average gain in RMSE due to splits on this variable. The sum of gain from all features is one.

A

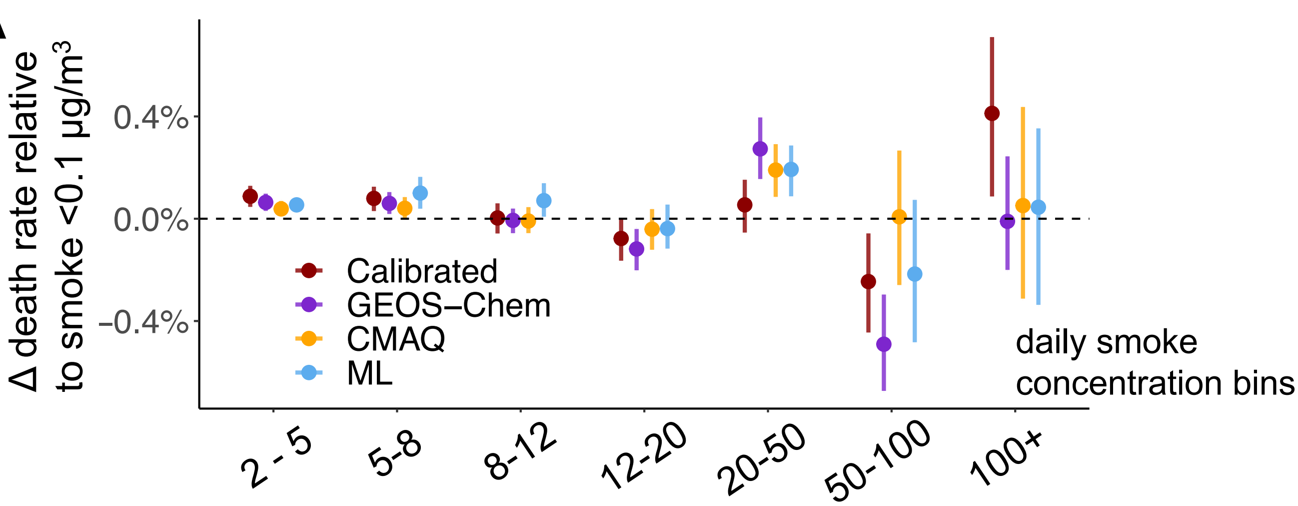

B Using dose-response function of # of days in smoke concentration bins

Outcome	Model	Mortality estimates
Annual deaths	CMAQ	37,658
Different DRFs	GEOS-Chem	16,599
	ML	55,213
	Calibrated	69,157
Annual deaths	CMAQ	58,254
Same DRF (from ML)	GEOS-Chem	27,301
	ML	55,213
	Calibrated	50,606

Figure S7: Empirically estimated dose-response functions using the number of days that fall in each smoke concentration bin in each year. Panel A shows the effects of exposure to one day of smoke $PM_{2.5}$ with different daily smoke concentrations (shown in the x-axis) relative to a day with smoke concentration of <2 $\mu g/m^3$, estimated using a Poisson model at the county and annual level using data from 2006–2020. The wildfire smoke data is the same across estimations in 2006–2019 (derived from the ML method), but is different in 2020 depending on the estimation approach. Panel B shows the estimated excess mortality due to smoke $PM_{2.5}$ in 2020 using different dose-response functions (DRF) and smoke $PM_{2.5}$ estimated by different methods. "annual deaths, different DRF" is estimated using the different DRFs shown in panel A. "annual deaths, same CRF" is estimated using the same DRF (derived from ML estimates) but different exposure estimates from four methods. Thus, the difference is only due to different wildfire smoke estimations. The error bars show the 95% confidence interval estimated using bootstrapping.